PERGAMON

International Journal of Heat and Mass Transfer 44 (2001) 4381–4389

International Journal of HEAT and MASS TRANSFER

www.elsevier.com/locate/ijhmt

Experimental study of the forces associated with mixed convection from a heated sphere at small Reynolds and Grashof numbers. Part I: cross-flow

G. Ziskind [a,*], B. Zhao [a], D. Katoshevski [b], E. Bar-Ziv [a,c]

[a] *Department of Mechanical Engineering, Ben-Gurion University of the Negev, P.O. Box 653, Beer-Sheva, Israel*
[b] *Department of Environmental Engineering, Ben-Gurion University of the Negev, P.O. Box 653, Beer-Sheva, Israel*
[c] *Institutes for Applied Research, Ben-Gurion University of the Negev, P.O. Box 653, Beer-Sheva, Israel*

Received 30 June 2000; received in revised form 13 March 2001

Abstract

The present paper addresses the issue of mixed convection from a small heated sphere in cross-flow configuration. The sphere is suspended in an electrodynamic chamber (EDC), where it is heated by a focused laser beam up to several hundred degrees above room temperature. As a result, there is free convection from the sphere, with the Grashof number smaller than 0.01. Then, a horizontal forced flow is applied and gradually increased in a quasi-static manner. Horizontal flow velocities are in the range 0–0.1 m/s, providing very low particle Reynolds numbers, usually less than 0.5. The effects of the free convection on the drag force, and of the forced flow on the free convection, are assessed measuring continuously the horizontal and vertical forces experienced by the sphere. It is shown quantitatively how the forced flow suppresses the free convection. A similarity law is suggested for the behavior of horizontal and vertical forces at various particle temperatures.

Keywords: Free and forced convection; Small sphere; Cross-flow

1. Introduction

Heat transfer from or to a body of spherical or near-spherical shape is a fundamental problem of great practical significance. It arises in such important industrial applications as fuel spray and coal combustion, fluidized beds, drying, particulate technologies, and many others in which small particles are involved. In general, free-, forced- and mixed-convection regimes are encountered there.

It is quite common to describe the magnitude of free convection in terms of Grashof or Rayleigh numbers that depend on the surrounding fluid properties, dimensions of the body in question, and the temperature difference between the body and the surroundings. In the applications mentioned above these numbers are usually quite small though the temperature difference may reach thousands of degrees. This is because the dimensions of the particles are small. As for the forced flow, the common parameter used there is the Reynolds number. The regime of heat transfer may be dominated by free convection, by forced convection, or represent comparable effects of both.

As discussed by Clift et al. [1], the dimensionless momentum equation for the mixed convection from a sphere includes the Grashof and Reynolds numbers, and also the dimensionless temperature. Since the flow associated with free convection is in the vertical direction, while the forced flow may have an arbitrary direction, the angle between the direction of the forced flow and the vertical direction becomes an additional parameter of the problem [2]. Thus, it is common to study the mixed convection analyzing three basic cases: (1) "assisting" regime, where the direction of the forced flow coincides with that of the free flow; (2) "opposing"

* Corresponding author. Tel.: +972-7-647-7089; fax: +972-7-647-2813.
E-mail address: gziskind@bgumail.bgu.ac.il (G. Ziskind).

0017-9310/01/$ - see front matter
PII: S0017-9310(01)00095-3

Nomenclature

d	particle diameter (m)
E	electric-field strength (N/C)
F	force (N)
g	gravitational acceleration (m/s^2)
Gr	Grashof number ($= g\beta[T_p - T_{cold}]d^3/\nu^2$)
h	heat transfer coefficient (W/m^2 K)
k	thermal conductivity (W/m K)
L	characteristic length (m)
Nu	Nusselt number ($= hd/k$)
Pr	Prandtl number
q	particle charge (C)
Q	volume flowrate (cm^3/min)
Re	Reynolds number ($= ud/\nu$)
T	temperature (K or °C)
u	velocity (m/s)
V	voltage (V)
x, z	Cartesian coordinates

Greek letters

β	thermal expansion coefficient (K^{-1})
μ	dynamic viscosity (kg/m s)
ν	kinematic viscosity (m^2/s)
ρ	density (kg/m^3)

Subscripts

cold	surroundings
f	film
fc	free convection
d	drag
e	electric
eff	effective
g	gas
p	particle
∞	ambient

regime, where the direction of the forced flow is opposite to that of the free flow; and (3) "crossing" regime, where the direction of the forced flow is normal to that of the free flow. Any other case may be analyzed based on the results for the three basic regimes.

The cross-flow regime of mixed convection is shown schematically in Fig. 1. One can see that if the forced flow is weak, the free convection dominates. It is characterized by a plume of upward-flowing fluid. On the other hand, when the forced flow is strong enough, it eliminates the free convection, and the flow around the hot sphere becomes similar to that around a cold one. While these two extreme situations are quite clear, the intermediate regimes for the cross-flow, or any other configuration in which the forced and free flows do not occur along the same axis, are rather complicated, and even a numerical solution presents great difficulty.

While free convection was studied quite extensively in the past, the existing results for mixed convection are rather limited, especially for small bodies where the Reynolds and Grashof numbers are small. A pioneering experimental work on the heat transfer from a sphere under combined free and forced convection was performed by Yuge [3], who suggested procedures for prediction of the Nusselt number. Hieber and Gebhart [4] studied mixed convection analytically, but their analysis concerns only the assisting and opposing flows. A work concerning a cylindrical geometry at small Reynolds and Grashof numbers was done by Nakai and Okazaki [5], who considered both pure and mixed convection from a heated horizontal thin wire. No numerical results exist in the literature on the cross-flow mixed convection from a heated sphere, in the relevant range of the Grashof and Reynolds numbers.

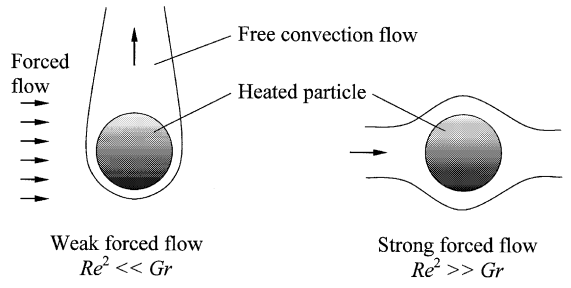

Fig. 1. Mixed convection from a heated sphere in the cross-flow.

In the present investigation, both free and forced convection from a spherical particle are studied in an electrodynamic chamber (EDC). Thus, it is in a sense an extension of the earlier work by Dudek et al. [6], who studied free convection only, using a similar device.

Recently we have developed a novel technique for the study of various physical phenomena related to a single small heated particle levitated in an EDC [7–9]. In the present work, this technique is applied to an experimental study of mixed cross-flow convection at small Grashof and Reynolds numbers. The regimes dominated by free and forced convection are considered along with the regimes where the contributions from free and forced convection are comparable to each other. The present work develops further the ideas and results obtained in the previous investigations by the authors [8,9]. These results will be discussed in connection with the findings of the present study.

2. Experimental method

The experimental system, shown in Fig. 2, and measurement procedure are well documented in the previous papers [8,9]. Thus, only the essential details are presented here.

2.1. Force balance on a levitated particle

A charged particle can be levitated by an electric field inside the EDC. Fig. 3 provides a schematic description of the force balance on a levitated charged particle in an electric field at various conditions. The design of the experimental apparatus enables one to uncouple the effects of different forces in the measurements, because the forces act in orthogonal directions. As a result, each force (weight, drag, photophoresis) could be balanced solely by the electric field that, in turn, can be directly measured.

As shown in Fig. 3, when only gravity, mg, which is directed downwards, is applied, the vertical electric force, $F_{ez} = qE_z$, balances the force of gravity, where m and q are the particle mass and charge, respectively, g is the gravitational acceleration, E denotes electric-field strength, and z is the vertical coordinate. The gas flows horizontally in the x-direction, hence the drag force F_d arising from that flow is uncoupled from the force of gravity and is balanced by the x-component of the horizontal electric force. A focused laser beam irradiates the particle, and free convection is generated, producing the upward directed force, F_{fc}, because the particle is hotter than its surroundings. The laser beam irradiates the particle horizontally in the y-direction, uncoupling the photophoretic force, F_{pp}, from the other forces.

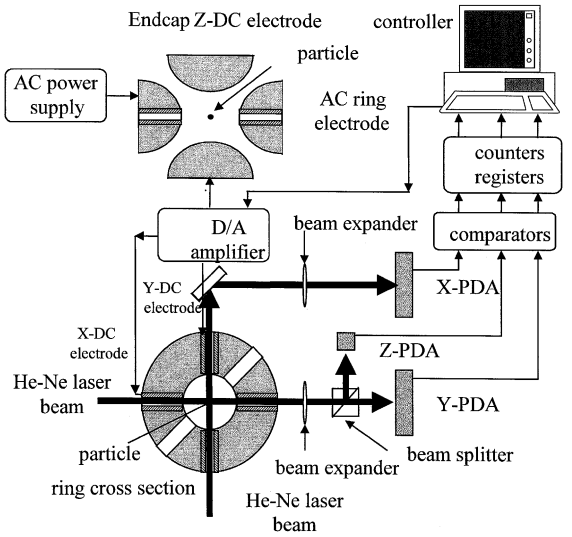

Fig. 2. Schematic description of the experimental set-up.

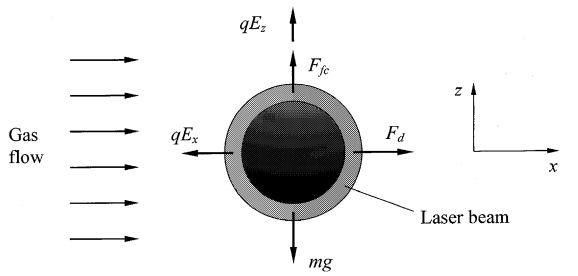

Fig. 3. Force balance on a levitated charged particle, with flow and irradiation in the horizontal plane and normal to each other.

2.2. Experimental set-up and procedure

Fig. 2, which was referred to previously, presents a schematic description of the experimental system. The position of a suspended particle is determined from the image of the particle in the Cartesian coordinates. A He–Ne laser beam traverses the particle and is projected onto a photodiode array (PDA), providing one coordinate axis. The second He–Ne laser beam, normal to the first, traverses the particle and splits into two beams that are projected onto two PDAs. The three PDA signals provide the x-, y-, and z-coordinates and determine the position of the particle.

A 3D-position controller is the central system in the EDC that is needed for weight and size measurements, stable heating, and for measuring changes in the force balance at each coordinate. This system consists of three parts: (1) an electro-optical sensing system; (2) a data acquisition system and an on-line tracing algorithm that determines the particle position; and (3) a proportional-integral-derivative controller. The three subsystems operate simultaneously in the x-, y-, and z-directions, using a computer.

One can realize the importance of the position controller if it is noted that the laser beam diameter is close to the particle size. Thus, a small drift of the particle from the beam focus upsets the heat balance. Uneven forces applied to a suspended particle (flow, radiation, evaporation, and buoyancy) can cause instabilities and loss of the particle. This major problem, encountered in previous models of the EDC, is overcome by using the 3D-position controller that maintains the particle at the center of the EDC. Another important feature of the new 3D system is its ability to operate without AC voltage, thus reducing further position variations. With the new developments, electric levitation is now ready for studying particles of arbitrary shape, with considerable forces applied in all directions, in a wide range of particle sizes and temperatures, for various flow velocities and ambient pressures.

In the current experiments, we use smooth spherical glassy-carbon particles, in the size range of 85–105 μm

diameter, because of their strong chemical resistivity to oxidation at the operating temperature range (300–600 K in the present work). Special attention is given to examining any changes in the particle mass and properties during the experiments. It is important to ensure that no change in particle size and properties occurs because of heating. We note here that the voltages required to levitate the particle at a fixed position can indicate the changes in its mass, thermal properties, porosity, etc. For this reason, for each levitated particle a special test is done, in which the laser power is increased linearly with time, then decreased at the same rate. This procedure is described in detail by Zhao et al. [8] and Katoshevski et al. [9].

A typical experiment is carried out in the following way. A particle is charged and levitated in the EDC to a fixed position. Its weight is balanced by the electric field in the z-direction, as shown in Fig. 3. Then, the particle is heated by a focused CO_2 laser beam to a certain level, depending on the applied laser power. During the heating process, there exists a very weak forced flow. The heating causes free convection around the particle that "reduces" the particle weight. Accordingly, the electric force in the z-direction is adjusted automatically in order to preserve the balance. Then, the nitrogen flow is started. The flow rate is increased very slowly, providing a quasi-static process, while the heating level is kept constant. The increasing drag force exerted on the particle is balanced by the electric field in the x-direction, see Fig. 3. It is important to note that the EDC controller maintains the particle at a fixed position regardless of the magnitude of the flow rate.

3. Results and discussion

3.1. Raw experimental data

Typical raw experimental results are shown in Figs. 4 and 5. The results are presented as measured in the experiment, i.e. voltage versus volume flow rate, for different laser power values. In the present experiments special care was given to high resolution with respect to the flow rate. For this reason, each curve presented in the figures contains about *two thousand* measured points. Since the results are quite similar for all the particles in the range 85–105 μm used in the experiments, we present here the results for an 88.5 μm particle. In every case, one curve (squares) represents the results for an unheated particle. The other curves represent five different heating levels, established by applying laser power of 2, 3, 4, 6, and 8 W. The flow rate inside the chamber varied from 0 to 50 cm^3/min.

Fig. 4 represents the voltage, V_x, needed to oppose the drag force, i.e. to keep a particle in the center when the forced flow is imposed in the horizontal direction. As

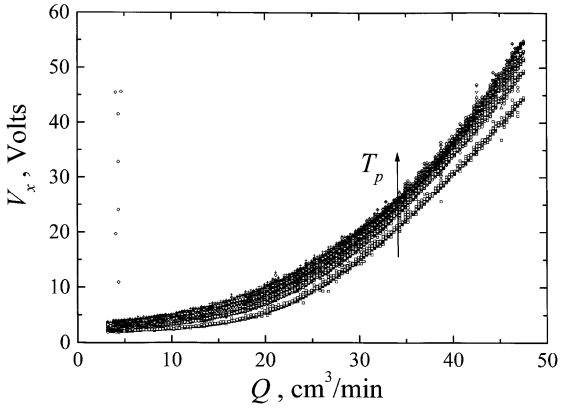

Fig. 4. The voltage V_x necessary to balance the drag force in the x-coordinate at different heating levels, as a function of flow rate: □ – no heating; ◯ – heating power of 2 W; △ – heating power of 3 W; ▽ – heating power of 4 W; ◇ – heating power of 6 W; + – heating power of 8 W. The same legend applies also to Figs. 5–9.

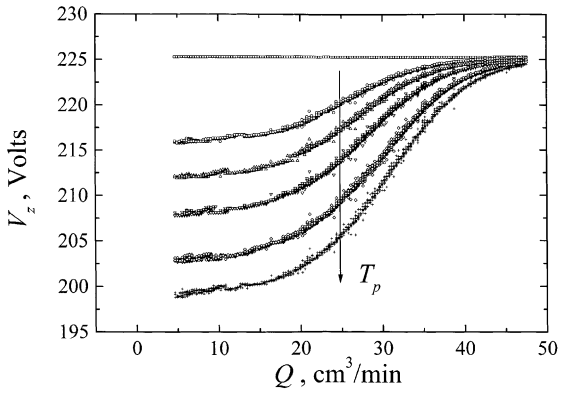

Fig. 5. The voltage V_z necessary to balance the weight and free-convection force in the z-coordinate at different heating levels, as a function of flow rate.

expected, the voltage increases as the volume flow rate, Q, increases, corresponding to an increase in drag force with flow velocity. This pattern is repeated for any heating level. On the other hand, for the same flow rate, the higher the heating level, the larger the drag and, accordingly, the voltage in the x-direction.

Fig. 5 shows the voltage, V_z, needed to keep the particle in the center. Since the drag and the gravity are orthogonal, for a cold particle the measured force in the z-direction is indeed not affected by the horizontal flow.

The heating process leads to a certain level of the particle temperature. One can see from Fig. 5 that, as the forced flow is close to zero, the voltage needed to keep the particle is minimal in every case. This situation corresponds to pure free convection. In other words, the

electric force F_{ez} and the free-convection force F_{fc} together balance the gravitational force mg, which is the only constant among the three forces mentioned.

Fig. 5 shows that as the forced flow increases, the vertical voltage needed to keep the particle increases. This is because the forced flow suppresses the free convection, causing F_{fc} to decrease and F_{ez} to increase in order to preserve the balance with respect to mg. Further increase in the forced flow eventually suppresses the free convection completely, and the balance reaches its asymptotic form $F_{ez} = mg$, i.e. the electric force approaches its value for the unheated particle. As shown in Fig. 5, the "heated" curves approach, with increasing forced-flow rate, the "cold" curve, in the order determined by the heating levels.

Summarizing the raw experimental results shown in Figs. 4 and 5, it is clear that (1) the drag acting on a heated sphere increases with the flow velocity, (2) the drag is larger, at the same velocity, as the heating level is higher, (3) the free convection is suppressed by the forced flow as the latter increases, and (4) the flow required to suppress the free convection completely depends on the heating level.

As mentioned above, Fig. 4 shows a similar increase in the drag force with velocity for different heating levels. Careful inspection of the results, however, will shortly reveal that this behavior is much more complicated. Fig. 6 shows the ratio of the voltage in the x-direction for a heated particle, V_x, to the voltage measured for the same particle without heating, $V_{x,\mathrm{cold}}$, for different heating levels versus the flow rate. This ratio represents the ratio of the drag force acting on a heated particle to the drag force acting on the same, but unheated, particle at the same flow velocity,

$$\frac{F_{\mathrm{d}}}{F_{\mathrm{d,cold}}} = \frac{V_x}{V_{x,\mathrm{cold}}}. \tag{1}$$

The ratio $V_x/V_{x,\mathrm{cold}}$, where the index "cold" indicates no heating by the laser, is obtained experimentally within uncertainty smaller than 0.4%. One can see that although, in general, the drag itself is larger for higher heating levels, the drag ratio does not behave monotonically, first increasing and then decreasing with the forced flow. The decrease in the ratio was revealed and explained in a previous investigation [9], using the concept of "effective diameter" which replaces the actual particle diameter at non-isothermal conditions. That approach will be discussed in the next section.

Fig. 7 represents the free-convection force normalized by the force of gravity. This ratio is measured in the EDC as

$$\frac{F_{\mathrm{fc}}}{mg} = \frac{V_{z,\mathrm{cold}} - V_{z,\mathrm{hot}}}{V_{z,\mathrm{cold}}}, \tag{2}$$

where the voltage difference in the numerator expresses the net force necessary to balance the free convection, while the voltage in the denominator balances the force of gravity.

The results of Fig. 7 reflect a number of essential features of the investigated phenomena. The force of free convection is larger when the heating level, and resulting particle temperature, is higher. This force is maximal at zero forced flow. At the same horizontal flow, expressed by the volume flow rate, the free-convection force is larger when the heating level is higher. As the flow increases, it suppresses the free convection, until the latter becomes negligible. A comparison of Figs. 6 and 7 shows that the free convection becomes practically undetectable at the same value of the volume flow rate where the drag force ratio ceases to decrease.

The free-convection force in the investigated range of particle temperatures reaches about 12% of the particle weight. Note that the maximal drag force experienced by

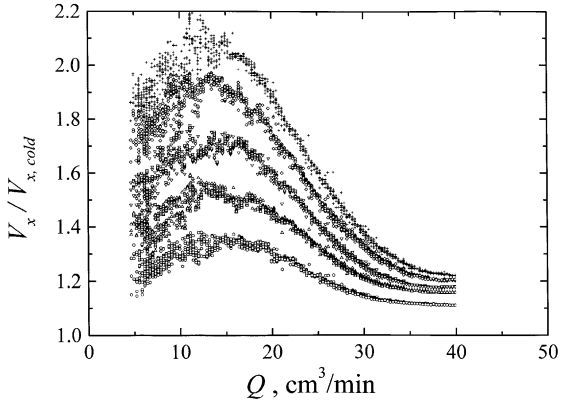

Fig. 6. The hot-to-cold drag force ratio at different heating levels, as a function of flow rate.

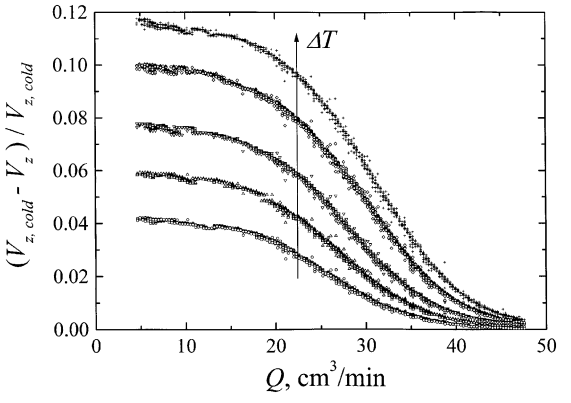

Fig. 7. The free-convection-to-weight ratio at different heating levels, as a function of flow rate.

the particle in our experiments was about 25% of the particle weight.

3.2. Dimensional analysis

We present here the results in a dimensionless form, convenient for generalization and analysis. For this purpose, the flow rate as measured in the experiments should be first replaced by the velocity. The procedure for velocity calibration was described in detail in previous investigations [8,9]. It is based on the well-known Stokes relation between the velocity and the drag force acting on a sphere at low Reynolds numbers, $Re_p = ud\rho_g/\mu_g < 0.5$,

$$F_d(T_\infty) = 3\pi d\mu_g(T_\infty)u, \tag{3}$$

where μ_g and ρ_g are the dynamic viscosity and density of the gas, respectively, d is the particle diameter, and u is the flow velocity when the particle is motionless. In this relation, it is implied that there is no difference between the particle temperature, T_p, and the temperature of the surrounding fluid, T_∞.

Assuming that the Reynolds numbers in our case are low, as is in fact shown later, Eq. (3) is used for velocity determination from the drag force. For an unheated particle, the ratio drag/weight is measured as the ratio $V_{x,\mathrm{cold}}/V_{z,\mathrm{cold}}$ where, as previously, the index "cold" indicates no heating. Since for a smooth sphere this ratio is given by $F_d/mg = 18\mu_g u/d^2\rho_p g$, the velocity is readily calculated from

$$u = \frac{\rho_p g d^2}{18\mu_g}\frac{V_{x,\mathrm{cold}}}{V_{z,\mathrm{cold}}}, \tag{4}$$

where $\rho_p = 1450\ \mathrm{kg/m^3}$ is the density of glassy-carbon particles. The ratio $V_{x,\mathrm{cold}}/V_{z,\mathrm{cold}}$ is measured continuously, with uncertainty smaller than 0.2%.

From the calibration, we obtain that, for the range of the volume flow rates used in the present investigation, $Q = 0$–$50\ \mathrm{cm^3/min}$, the velocity was in the range $u = 0$–$12\ \mathrm{cm/s}$.

In previous investigations [8,9] we have discussed the possibility of temperature estimation from Eq. (3). Since the only parameter in it that depends on the temperature is the viscosity, the latter can be calculated from Eq. (3) for a hot particle. It could be done, however, only when the free convection is suppressed by the forced flow completely. As shown in the previous studies, when the forced flow dominates, the Stokes relation can be used in a slightly modified form,

$$F_d(\Delta T) = 3\pi d\mu_g(T_{\mathrm{film}})u, \tag{5}$$

where $\Delta T = T_p - T_\infty$, T_{film} is the film temperature given by $T_{\mathrm{film}} = (T_p + T_\infty)/2$, and u is the velocity at which the free convection is completely suppressed by the forced flow. It is important that the flow is still in the Stokes regime. Hence, if the forces are known, the viscosity at an elevated temperature, $\mu_g(T_{\mathrm{film}})$, can be calculated. The viscosity of a gas, as a function of temperature, can be expressed by a second-order polynomial [10]:

$$\mu_g = 3.983\times10^{-6} + 4.966\times10^{-8}T - 1.346\times10^{-11}T^2, \tag{6}$$

where the temperature is in Kelvin and the viscosity is in kg/m s. Hence, the film temperature is estimated from Eq. (6), leading to particle temperature T_p.

Using this approach, the particle temperature levels were estimated for the sphere of 88.5 μm diameter. These temperatures, listed in Table 1, correspond to the curves in Figs. 4–7.

The decrease in the drag force ratio with the flow velocity, see Fig. 6, has been explained previously [9]. The drag force acting on a heated particle was assumed to behave as

$$F_d(d,\Delta T,u) = 3\pi d_{\mathrm{eff}}(d,\Delta T,u)\mu_g(T_{\mathrm{film}})u, \tag{7}$$

where $d_{\mathrm{eff}}(d,\Delta T,u)$ is an "effective diameter" that depends on the actual particle diameter, temperature difference, and on the flow velocity. We note here that Eq. (5) is, essentially, a reduced form of Eq. (7) for the case $d_{\mathrm{eff}} = d$.

The concept of effective diameter is based on physical considerations, which are briefly summarized here. When a particle is hotter than its surroundings, a free-convection flow around the particle is generated. Thus, the forced cross-flow encounters an obstacle that is effectively larger than the particle itself. From a certain velocity value, this effective diameter reduces and tends to approach the actual particle diameter, because the

Table 1
Experimental parameters for the particle 88.5 μm in diameter

Laser power P (W)	Particle temperature T_p (K)	Grashof number Gr_f	Characteristic Reynolds number $Re_f = Gr_f^{1/2}$
2	395	0.0045	0.067
3	430	0.0049	0.070
4	455	0.0050	0.071
6	490	0.0051	0.071
8	520	0.0051	0.071

free convection is suppressed by the forced flow. In this situation, Eq. (7) becomes similar to Eq. (3), with the only difference that the viscosity should be taken at the film temperature instead of the room temperature. While this concept has proved itself in the previous analysis, it cannot be used to explain the initial increase in the drag ratio.

As shown above, the temperature levels were estimated for the case where the free convection was fully suppressed by the forced flow. It is important to know whether the particle temperature is the same for the free-convection-dominated and intermediate regimes. In other words, one must be sure that the particle is not just cooled by the forced flow when the latter increases.

For a steady state, the heat transfer rate is determined by laser irradiation, which is constant for any given experiment. Thus, the temperature difference is determined by the heat transfer coefficients, which for pure forced and free convection are given, respectively, by [11]

$$Nu_{\mathrm{f}} = 2 + 0.6Re_{\mathrm{f}}^{1/2}Pr_{\mathrm{f}}^{1/3} \tag{8a}$$

and

$$Nu_{\mathrm{f}} = 2 + 0.6Gr_{\mathrm{f}}^{1/4}Pr_{\mathrm{f}}^{1/3}, \tag{8b}$$

where $Nu = hd/k$ is the Nusselt number, $Re = ud/v$ is the Reynolds number, $Gr = g\beta(T_{\mathrm{p}} - T_{\mathrm{cold}})d^3/v^2$ is the Grashof number, Pr is the Prandtl number, h is the heat transfer coefficient, k is the thermal conductivity, v is the kinematic viscosity of the gas, and β is the coefficient of thermal expansion. It is important that all the properties are evaluated at the film temperature, denoted by index f.

The free convection in our experiments is suppressed completely at $Re_{\mathrm{f}} \approx 0.3$–$0.4$, yielding from Eq. (8a) the Nusselt number of $Nu \approx 2.3$, which is quite close to the asymptotic value of $Nu = 2$ for pure conduction. An estimation based on Eqs. (8a) and (8b) shows that the Nusselt number is almost constant in our experiments, while the drag force varies considerably. The effect of mixed convection on the Nusselt number and the drag at $Re < 1$ was first discussed by Clift et al. [1] (for assisting and opposing regimes), with the same conclusions. The temperature difference above the surroundings, $T_{\mathrm{p}} - T_{\infty}$, for the particle cooled by free convection only, could exceed the temperature difference, $T_{\mathrm{p}} - T_{\infty}$, for the same particle under pure forced convection, by no more than 5%. This deviation is actually smaller, taking into account additional cooling by radiation. Thus, the particle temperature remains almost the same at all the stages of the process.

In order to compare the effects of free and forced convection, it is common to use the ratio of the Grashof number to the squared Reynolds number, Gr/Re^2, which appears in the dimensionless form of the momentum equation [1],

$$\frac{Gr}{Re^2} = \frac{\beta g(T_{\mathrm{p}} - T_{\infty})d}{u^2}. \tag{9}$$

The values of the Grashof number, based on the estimated temperatures, are listed in Table 1. The thermal expansion coefficient β was taken at the film temperature.

One can see that the film-temperature Grashof number is almost the same over the given range of particle temperatures. Thus, a small deviation of the particle temperature from the estimated value does not have any effect on it. Because of such behavior of the Grashof number, the characteristic film-temperature Reynolds number, defined from $Re_{\mathrm{f}}/Gr_{\mathrm{f}}^{1/2} = 1$, is almost constant. The points at which $Re_{\mathrm{f}} = Gr_{\mathrm{f}}^{1/2}$ for different temperatures, as listed in Table 1, separate the region of stronger free convection from that of the stronger forced one.

As mentioned previously, the dimensionless momentum equation for buoyancy-driven flows [1] includes, along with the Reynolds and Grashof numbers, the dimensionless temperature difference. This difference determines the free-convection velocity field and, as a result, affects the mixed-convection velocity field and the forces acting on the sphere. The effect of free convection is stronger when particle temperature is higher.

Therefore, the relative temperature difference $(T_{\mathrm{p}} - T_{\mathrm{cold}})/T_{\mathrm{cold}}$ can be applied to the analysis of the results. As shown in Fig. 8, the representation of the free-convection force as $[F_{\mathrm{fc}}/F_{mg}]/[(T_{\mathrm{p}} - T_{\mathrm{cold}})/T_{\mathrm{cold}}]^{5/4}$ versus Re_{f} merges the curves into a single one, providing a 5/4-power law for data generalization.

As discussed above, when free convection becomes fully suppressed by the forced flow, the drag force ratio tends to the ratio of the viscosities, $F_{\mathrm{d}}/F_{\mathrm{d,cold}} \to \mu_{\mathrm{f}}/\mu_{\mathrm{cold}}$. One may assume that, at the entire range of $0 < Re < 0.5$, the drag force along the flow direction is a superposition of two factors, namely, the Stokes-like

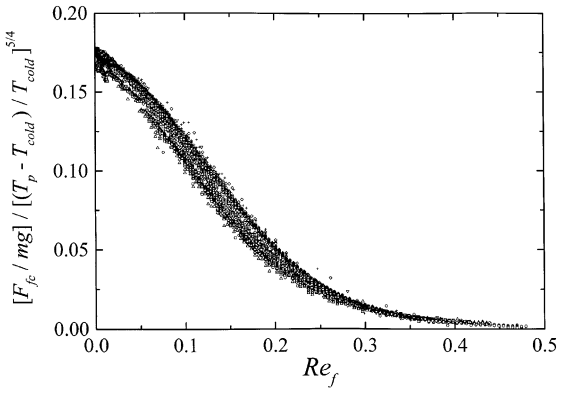

Fig. 8. The temperature-normalized free-convection force, as a function of the "film" particle Reynolds number.

drag based on the film temperature, and the additional force arising from free convection:

$$F_{\mathrm{d}} = 3\pi d\mu_{\mathrm{g}}(T_{\mathrm{film}})u + F_{\mathrm{d,free}}. \tag{10}$$

Dividing Eq. (10) by $F_{\mathrm{d,cold}} = 3\pi d\mu_{\mathrm{g}}(T_{\infty})u$ and rearranging terms, one obtains the contribution of free convection to the forced-flow drag as

$$\frac{F_{\mathrm{d,free}}}{F_{\mathrm{d,cold}}} = \frac{F_{\mathrm{d}}}{F_{\mathrm{d,cold}}} - \frac{\mu_{\mathrm{g}}(T_{\mathrm{film}})}{\mu_{\mathrm{g}}(T_{\infty})}. \tag{11}$$

Based on this result and the finding for free convection above, the 5/4-power law can be applied also to the analysis of the drag force as a function of the particle temperature. Fig. 9 presents the generalized data in the form $[F_{\mathrm{d}}/F_{\mathrm{d,cold}} - \mu_{\mathrm{f}}/\mu_{\mathrm{cold}}]/[(T_{\mathrm{p}} - T_{\mathrm{cold}})/T_{\mathrm{cold}}]^{5/4}$ versus Re_{cold}. Note that for F_{fc} the best fit has been obtained versus Re_{f}. One can see once again that all the measured points tend to form a single curve, notwithstanding the heating level.

Inspection of the results of Figs. 8 and 9 indicates that the free-convection influence becomes almost invisible at $Gr_{\mathrm{f}}/Re_{\mathrm{f}}^2 \approx 0.02$–$0.03$. This is in good agreement with the finding of Yuge [3] that natural convection is of negligible influence on heat transfer at $Gr/Re^2 < 0.01$. The latter fact is important also for application of the present results to any situation in which free convection from a sphere is suppressed by the forced flow in the Stokes regime. Recall that the particles used in the present study were 80–100 μm in diameter. In our opinion, the results of the present study are true also for smaller particles at much higher temperatures. This is because the Grashof number decreases with the particle diameter to the third power. Thus, for a micrometer-sized particle the Grashof number is very small even for a very high particle temperature. As a result, the forced flow, strong enough to suppress the free convection, remains Stokesian. Therefore, the interdependence of free and forced convection is similar to that found and analyzed in the present study.

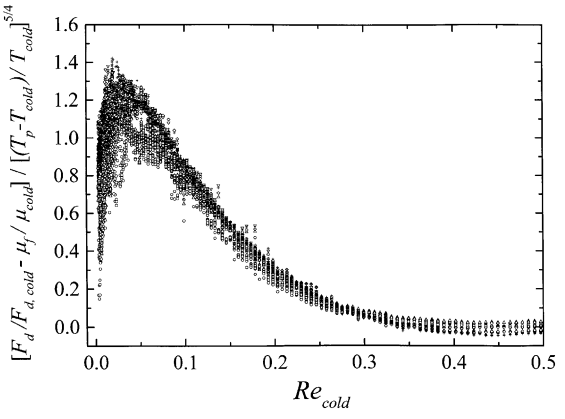

Fig. 9. The temperature-normalized drag force ratio, as a function of the "cold" particle Reynolds number.

4. Closure

The present investigation provides novel qualitative and quantitative results concerning the complex issue of mixed convection in the cross-flow around a sphere. It is shown how the free and forced convection interact both when one of them dominates the other, and when there are comparative contributions of both.

A power law is established for generalization of the results concerning both the hydrodynamic drag force acting on a heated particle, and the force resulting from the free-convection flow around the particle. This law is applicable to a wide range of particle sizes and temperatures.

The results of the present study can be applied to various systems where the temperature difference between the particles and the gas should be taken into account in the analysis.

Acknowledgements

This study has been partially supported by US–Israel Binational Science Foundation (BSF) grant number 97-00030.

References

[1] R. Clift, J.R. Grace, M.E. Weber, Bubbles, Drops, and Particles, Academic Press, New York, 1978.
[2] G.D. Raithby, K.G.T. Hollands, Natural convection, in: W.M. Rohsenow, J.P. Hartnett, E.N. Ganic (Eds.), Handbook of Heat Transfer Fundamentals, second ed., McGraw-Hill, New York, 1985.
[3] T. Yuge, Experiments on heat transfer from spheres including combined natural and forced convection, ASME J. Heat Transfer 82 (1960) 214–220.
[4] C.A. Hieber, B. Gebhart, Mixed convection from a sphere at small Reynolds and Grashof numbers, J. Fluid Mech. 38 (1969) 137–159.
[5] S. Nakai, T. Okazaki, Heat transfer from a horizontal circular wire at small Reynolds and Grashof numbers – I: pure convection, II: mixed convection, Int. J. Heat Mass Transfer 18 (1975) 387–413.
[6] D.R. Dudek, T.H. Fletcher, J.P. Longwell, A.F. Sarofim, Natural convection induced drag forces on spheres at low Grashof numbers: comparison of theory with experiment, Int. J. Heat Mass Transfer 31 (1988) 863–873.
[7] X. Zhang, E. Bar-Ziv, Theoretical analysis and measurement of 3-D electrodynamic field: direct measurement of 3-D force balance applied on a suspended particle, Meas. Sci. Tech. 7 (1996) 1713–1720.

[8] B. Zhao, D. Katoshevski, E. Bar-Ziv, Temperature determination of single micrometre-sized particles from forced/free convection and photophoresis, Meas. Sci. Tech. 10 (1999) 1222–1232.
[9] D. Katoshevski, B. Zhao, G. Ziskind, E. Bar-Ziv, Experimental study of the drag force acting on a heated particle, J. Aerosol Sci. 32 (2001) 73–86.
[10] Y.S. Touloukian, C.Y. Ho, in: Thermophysical Properties of Matter, The TPRC Data Series, vol. 3., Thermophysical Properties Research Center, Purdue University, 1970.
[11] R.B. Bird, W.E. Stewart, E.N. Lightfoot, Transport Phenomena, Wiley, New York, 1960.